ELSEVIER

Ceramics International 28 (2002) 337–344

CERAMICS INTERNATIONAL

www.elsevier.com/locate/ceramint

Injection moulding and sintering of ceria ceramics

Karel Maca*, Martin Trunec, Jaroslav Cihlar

Department of Ceramics, Brno University of Technology, Technicka 2, 616 69 Brno, Czech Republic

Received 28 May 2001; received in revised form 20 June 2001; accepted 18 July 2001

Abstract

Ceria powder was dry-milled to sub-micrometric particle sizes and used in the preparation of ceramic mixture for injection moulding. Specimen bodies were injection moulded in the shape of rectangular bars. The sintering kinetics of these bodies was studied in air atmosphere under various sintering conditions and also by the rate-controlled sintering method. Sintering the injection moulded CeO_2 to a density of 7.08 g cm^{-3} (99.3% TD) was possible already at a temperature of 1400 °C, and the highest density value (99.8% TD) was obtained at a heating rate of 2 °C min^{-1} and a holding time of 1 h at 1500 °C. Using heating rates of over 5 °C min^{-1} had an adverse effect on the density obtained. Applying the rate-controlled sintering (RCS) method did not lead to any decrease in the grain size if compared with temperature-controlled sintering (TCS). No reduction of CeO_2 ceramics was observed during all sintering experiments.

Keywords: A. Injection moulding; A. Sintering; B. Grain size; D. CeO_2

1. Introduction

Ceramic materials based on CeO_2 have recently grown in significance as a material holding much promise for the production of electrolyte for solid oxide fuel cells (SOFCs). Ceria-based electrolytes are of better ion conductance than yttria-stabilized zirconia used up to now [1–6]. This makes it a favourite material for the production of fuel cells that work at lower temperatures (600–800 °C) than zirconia-based SOFCs (800–1000 °C). Other application possibilities of ceria ceramics embrace gas sensors, petroleum-cracking catalysts, oxygen storage medium in three-way car converters, and electrochemical cells.

Papers have recently been published that treat the preparation of pure cerium dioxide [7–14] and cerium dioxide doped with rare earth elements or other bivalent or trivalent cations (Gd, Sm, Ga, Y, Co, Ca, ...) [1–7,9,11,14). Different methods (hydrothermal synthesis, electrochemical synthesis, precipitation, ...) were used to prepare both nanometric [6–14] and sub-micrometric [1–5,7,8,10] particles. Ceramic powders produced in this way were then moulded, most frequently by uniaxial pressing [1,4,5,7–10,14] complemented sometimes with cold isostatic pressing [2,3,6,11–13], into simple shapes with subsequent sintering, in order to provide for the description of sintering kinetics of this material. Sintering kinetics of the ceramic green body does not only depend on the composition and size of powder material but also, at least to the same extent, on the arrangement of particles and pores in the ceramic green body [15,16].

The literature brings only sporadic data on the shaping of ceria-based ceramics by other than uniaxial and isostatic pressing methods. Van Herle et al. [4,17] examined the possibility of shaping yttria-doped ceria by the tape casting method while Zhitomirsky [18] used the method of electrophoretic deposition. One of the possible ways of producing economically ceramics of complex shapes is either extrusion or injection moulding of plastic ceramic mixtures. In this area, however, no work has so far been published that would concern ceria-based ceramics.

It has been the aim of the present work to verify the possibility of preparing ceramic bodies from sub-micrometric cerium dioxide by the injection moulding method, and to study sintering kinetics and grain growth of ceramics prepared in the above way.

2. Experimental

Ceria powder (Guangzhou Zhujiang Refinery, China) of 99.95% CeO_2 purity was used for the preparation of

* Corresponding author. Fax: +420-5-4114-3202.
E-mail address: maca@zam.fme.vutbr.cz (K. Maca).

0272-8842/02/$22.00
PII: S0272-8842(01)00100-6

ceramic mouldings. Ceria powder was treated by milling in a ball mill in the presence of stearic acid for a period of 24 h. The particle size distribution of the ceramic powder prior and subsequent to the treatment was determined on a laser diffraction analyzer (LA-500, Horiba, Japan). The ceramic suspension for injection moulding contained 89.8 wt.% of cerium dioxide, 4.8 wt.% of copolymer ethylene-vinylacetate (Elvax 250, Du Pont de Nemours, USA), 3.2 wt.% of paraffin wax (R-54/56, Slovnaft, Slovakia), and 2.2 wt.% of stearic acid (1.00671 Merck, Germany). The powder loading in ceramic suspension was 53 vol%. The suspension was prepared by mixing the treated ceramic powder with the other binder components in a heated two-blade kneader (HKD 0.6, IKA-Labortechnik, Germany) at a temperature between 110 and 120 °C for a period of 2 h. Rheological behaviour of the ceramic suspension was established on a capillary rheometer (Galaxy V, Kayness, USA). The measurement was performed within the shear-rate range from 10^2 to 10^3 s^{-1} at temperatures of 100–160 °C. Shear-rate values were recalculated for the non-Newtonian behaviour of mixtures by means of the Weissenberg-Rabinowitsch method [19].

Specimens in the shape of prisms (3.5×4.65×60 mm) were prepared by injection moulding (Allrounder 220M, Arburg, Germany). The temperature of injected mixture was 160 °C, the mould temperature was 25 °C. The binder was removed in nitrogen atmosphere at a heating rate of 10 °C h^{-1} up to a temperature of 500 °C. During binder removal the bodies were embedded in activated carbon. After debinding the bodies were presintered in air atmosphere at a temperature of 800 °C for 1 h. The density of bodies after presintering at 800 °C/1h and after high-temperature sintering was determined on the basis of Archimedes' principle, with distilled water as the fluid medium (EN 623-2). The specimens were sintered in an L70/1700 high-temperature dilatometer (Linseis, Germany) with vertical specimen orientation. All sintering experiments were performed in air atmosphere. For the study of sintering kinetics, different temperature modes were chosen: temperature-controlled sintering (TCS) with a constant heating rate of 2, 5 and 10 °C min^{-1} up to the sintering temperature (1400, 1450 and 1500 °C), at which temperature there was a holding time (of 40 min to 4 h), and rate-controlled sintering (RCS) [20,21].

On the curves giving the temperature dependence of specimen shrinkage $\varepsilon = f(T)$, some significant points were determined, which characterize sintering kinetics of the bodies, namely the temperature of shrinkage onset, the temperature of maximum shrinkage rate, and the temperature of shrinkage slow-down. The method of determining these points is given in detail in Maca et al. [22].

The temperature dilatation of material, which was established from the cooling curves of sintered specimens, was subtracted from the shrinkage values. The time and temperature dependence of shrinkage $\varepsilon = f(t, T)$ was then recalculated to give the time and temperature dependence of relative density $\rho_{rel} = f(t, T)$. For the transformation from shrinkage to density the final densities of ceramic specimens measured after sintering were used because they could be measured with greater precision than the green densities. After sintering, the specimens were cut transversely and polished by standard ceramographic methods and thermally etched in air at 1400 °C/5 min to make the grain boundaries more pronounced. The average grain size of sintered ceramic materials was determined by the linear intercept method (LIM). For each specimen a total of 15 line segments were evaluated. Pictures obtained by a scanning electron microscope (XL30, Philips, the Netherlands) were used as the basis of grain size evaluation.

3. Results and discussion

3.1. Particle shape and size

Fig. 1 gives the microphotograph of particles of as-received ceria powder. Powder particles were formed by clusters of cracked grains, which were up to 10 μm in size. These particle size values of cerium dioxide powder were confirmed by particle size measurement (Fig. 2). Powder with the above structure of particles was not suitable for the preparation of thermoplastic ceramic mixture for injection moulding of compact ceramics [23]. That is why the green powder material was treated by milling in a ball mill. Fig. 3a, b give the microphotographs of CeO_2 particles subsequent to treatment in the ball mill. It is obvious that the original grains (Fig. 1) were broken into individual compact pieces of less than 0.5 μm in size (Fig. 3b). During milling in the presence of stearic acid, however, large agglomerates (of up to 50 μm in size) of tiny particles were formed (Fig. 3a). After milling the powder, the particle size, established by laser diffraction, was only 0.37 μm, with the largest particles not exceeding 1.5 μm (Fig. 2). This is to say that at the time the particle size

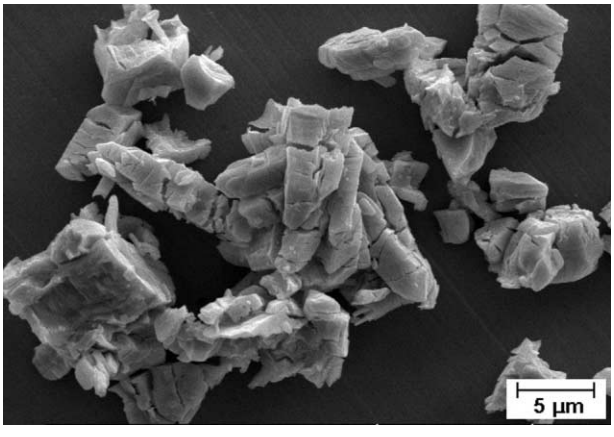

Fig. 1. SEM micrograph of the as-received ceria powder.

was being measured, all the large agglomerates observed in microphotographs were thoroughly broken up by either ultrasonic washing or dissolution in the carrier medium (ethanol).

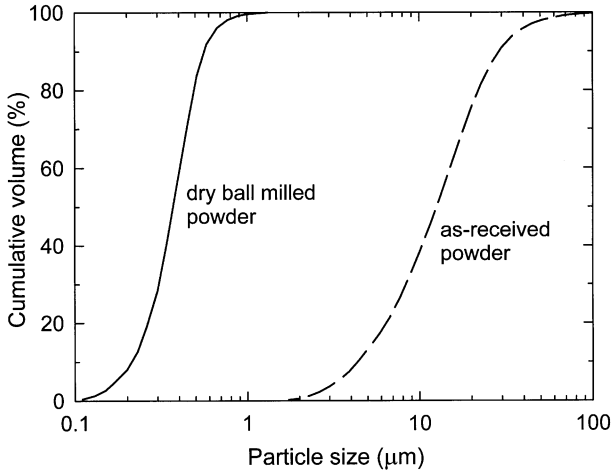

Fig. 2. Particle size distribution of as-received and dry ball milled ceria powder.

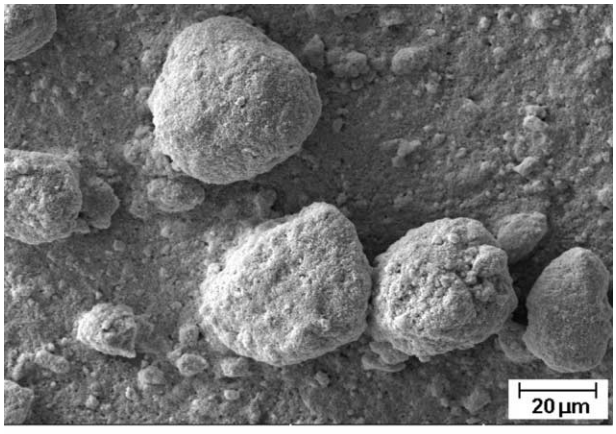

(a)

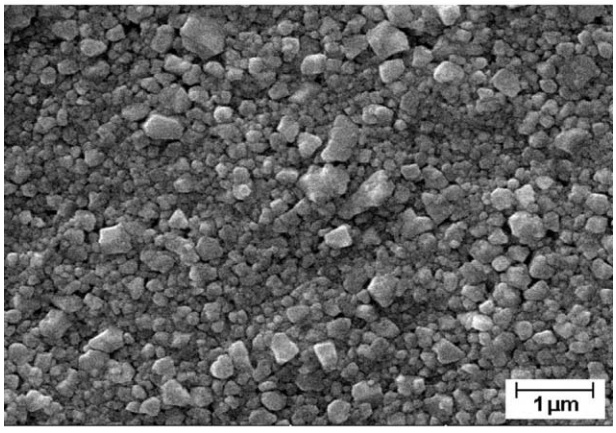

(b)

Fig. 3. SEM micrographs of dry ball milled ceria powder showing (a) large soft agglomerates present after milling and (b) size and shape of individual particles.

3.2. Ceramic mixture rheology

Fig. 4 gives the dependence of viscosity on shear rate at temperatures of 100–160 °C for the ceramic mixture under study. Over the whole range of the temperatures examined, the ceramic mixture showed pseudoplastic behaviour, i.e. viscosity decreased with increasing shear rate. The dependence of shear stress on shear rate was described by the power law [24]:

$$\eta = K \cdot \dot{\gamma}^{(n-1)}, \tag{1}$$

where η is the mixture viscosity, K is the constant, $\dot{\gamma}$ is the shear rate, and n is the exponent giving the deviation from Newtonian behaviour. The model chosen was in good agreement with the values measured ($r^2 > 0.99$). The exponent of power law, n, for the individual temperatures ranged from 0.30 to 0.38, the average value being 0.34. The temperature dependence of the ceramic mixture viscosity for shear rates of 200 and 1000 s^{-1} can be seen in Fig. 5. The activation energy values of viscous flow were established with the aid of the Andrade relation [24]

$$\eta = A \cdot e^{\frac{E}{RT}}, \tag{2}$$

where A is the constant, E is the activation energy of viscous flow, R is the universal gas constant, and T is the absolute temperature. The activation energy was calculated to be 15.0 kJ mol^{-1} for the shear rate 200 s^{-1}, and 12.9 kJ mol^{-1} for the shear rate 1000 s^{-1}.

Comparing the obtained viscosity values of CeO_2 ceramic mixture with standard alumina mixture for injection moulding with the same proportion of ceramic phase [25], we find that in the case of ceria the viscosity was 4–5 times higher. In comparison with alumina ($d_{50} = 0.60$ μm) the ceria powder used exhibited particles of almost halved size. This can explain the higher viscosity of CeO_2 ceramic

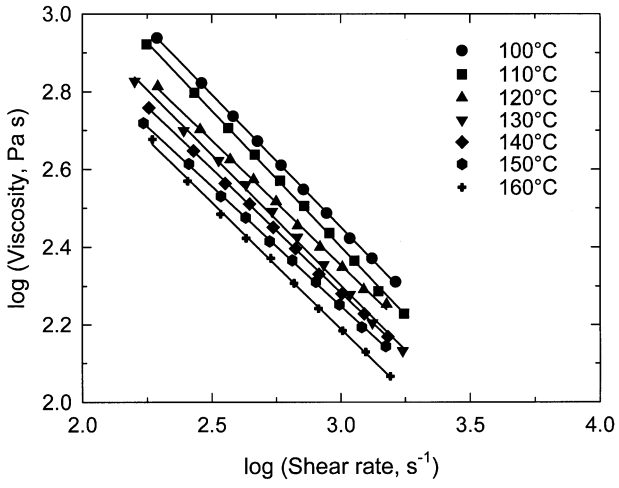

Fig. 4. Rheological behaviour of ceria mixture at different temperatures.

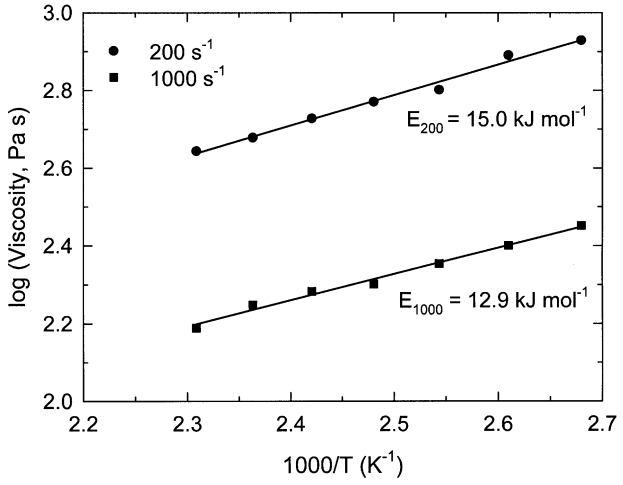

Fig. 5. The temperature dependence of viscosity of ceria mixture at shear rates of 200 and 1000 s^{-1}.

mixture, which was rather similar to mixtures with fine tetragonal ZrO_2 ($d_{50} = 0.45$ μm) [26]. Unlike the alumina mixture and most of the ZrO_2 mixtures, however, the ceria mixture exhibited higher pseudoplasticity (a lower exponent n) and a less steep temperature dependence of viscosity (a lower activation energy). Of a similar nature are, for example, mixtures of ZrO_2 with a powder treated by milling in a ball mill [26]. It can be assumed that the same as with ZrO_2, with CeO_2 too, agglomerates may have remained in the mixture after mixing, which were formed during milling (and which disintegrated during particle measurement and were therefore not found). Due to the high shear rates, these agglomerates got aligned or broken up in the rheometer.

3.3. Relative density of CeO_2 ceramics prior to sintering

The density of injection moulded CeO_2 ceramics after presintering at 800 °C/1h was 4.87 g cm^{-3}. Taking into consideration the theoretical density of CeO_2, $\rho_{theor} = 7.132$ g cm^{-3}, we obtain an average relative green density of specimen bodies, $\rho_{rel0} = 68.3\%$ (the standard deviation from 12 measurements was 0.2%). The relative proportion of open pores (defined as the ratio of the volume of pores open towards the body surface and the total body volume inclusive of open and closed pores) was 31.5%. The bodies thus contained a negligible proportion (0.2%) of closed (unsoaked) pores. Different values of theoretical density of CeO_2 can also be found in the literature; for example, Zhou et al. [8] gives the value 7.184 g cm^{-3}. He obtained this value by calculation from the measured value of ceria lattice parameter (0.5419 nm). The most frequently published values of the ceria lattice parameter range from 0.5409 to 0.5411 nm [27–29], which would correspond to a theoretical density of 7.22 g cm^{-3}. In view of the non-stoichiometry of CeO_{2-x}, which is due to oxygen vacancies and not to cerium interstitials [28], the real density is, however, lower than the crystallographic density. In the present work we will use the frequently given value of theoretical density of ceria, namely $\rho_{theor} = 7.132$ g cm^{-3} [12,29,30].

The relative density of presintered specimen bodies was higher than 68%, which for injection moulded bodies prepared from sub-micrometric powders is a very high value, the more so if we consider that the powder filling of ceramic suspension made only 53.5 vol.%. No similarly effective arrangement of presintered bodies could be achieved in any of the eight types of specimen studied in [22]—Al_2O_3, ZrO_2, ZTA and ATZ prepared on the one hand by injection moulding and on the other by isostatic pressing of sub-micrometric powders. A certain similarity could be found in injection-moulded ZrO_2. The ceramic suspension prepared with milled zirconia powder had a volume filling of 52.5%. After removing the binder and after presintering, the density of ZrO_2 green bodies increased to ca. 62.5% [22], while in the case of non-milled powder a powder loading of the suspension of 50.5% only led to a relative green body density of $\rho_{rel0} = 51.3\%$. These results correlate with the results of viscosity measurement given above, and they support the hypothesis of the formation of agglomerates during milling. As long as these agglomerates were of small inner porosity, they were able to favourably affect the density of presintered bodies.

3.4. Sintering kinetics of injection moulded CeO_2

The final relative density obtained in all sintering experiments is given in Table 1, inclusive of sintering conditions. All temperature modes led to densities higher than 99% TD, even a specimen sintered at a temperature of 1400 °C (holding time 4 h) reached a final relative density of 99.3%. Fig. 6 gives the shrinkage curves of specimens sintered at heating rates of 2 °C min^{-1} (holding time of 1 h at 1500 °C), 5 C min^{-1} and 10 °C min^{-1} (holding time in these two cases was 2 h at 1500 °C). Shrinkage in all the three specimens was very similar, the differences in the shape of individual curves

Table 1
Relative density (ρ_f), standard deviation (s) and number of measurements (n) of sintered CeO_2 ceramics

Heating rate (°C min^{-1})	Sintering temperature/holding time (°C)/(h)	ρ_f (%)	s (%)	n (–)
5	1400/4	99.28	0.03	3
5	1450/3	99.57	0.03	3
5	1500/2	99.71	0.05	3
5	1500/0.67	99.52	0.03	3
10	1500/2	99.34	0.08	3
2	1500/1	99.75	0.03	3
RCS		99.51	0.08	3

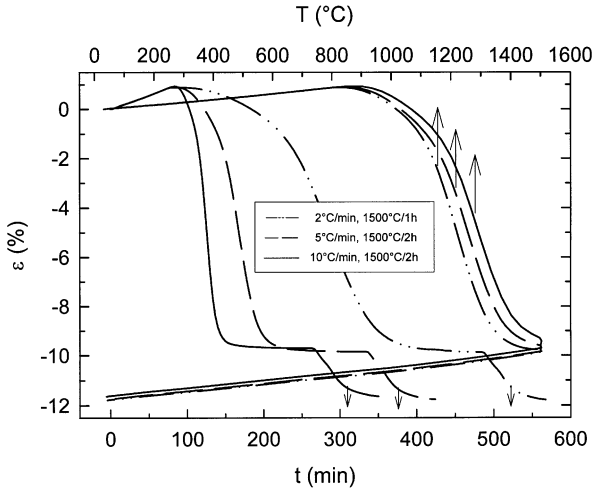

Fig. 6. The dependence of relative shrinkage of injection moulded ceria on temperature and time at different heating rates.

could be explained by different rates of heating since slower heating meant, of course, a longer exposure in the given temperature interval. The difference in the resultant shrinkage was more significant. The specimen sintered at a rate of 10 °C min^{-1} exhibited a smaller resultant shrinkage (−11.64%) than the specimens sintered at rates of 5 °C min^{-1} (−11.77%) and 2 °C min^{-1} (−11.80%), which corresponded to the final relative densities reached (99.3% vs 99.7% and 99.8%). It followed from the values of time dependence $\varepsilon = f(t)$ given in this graph that after two hours at 1500 °C the specimen heated at a rate of 10 °C min^{-1} was shrinking at a rate of −0.02% h^{-1}, which is to say that even a longer holding time at the sintering temperature would not lead to any pronounced increase in density. In contrast to the sub-micrometric ceria used here, Zhou and Rahaman [7] reported for nanometric CeO_2 the same course of densification for heating rates of 1, 5 and 10 °C min^{-1}.

The curves giving the dependence of relative shrinkage on temperature $\varepsilon = f(T)$ were also used to evaluate some significant parameters of sintering kinetics. Table 2 gives the temperatures of shrinkage onset (T_1), the temperature of maximum rate of shrinkage (T_2) inclusive of this maximum rate shrinkage (v_{max}) and the temperature of slowed-down sintering (T_3) as established by analyzing the shrinkage curves of CeO_2 ceramics. Individual temperature values were different for different temperature gradients, they increased with the rate of heating. A comparison of the sintering parameters of ceria and those of alumina, ZrO_2, ZTA and ATZ prepared on the one hand by injection moulding and, on the other hand, by isostatic pressing of sub-micrometric powders [22] is given in Table 3. The specimens were sintered at a rate of 5 °C min^{-1}. Cerium dioxide exhibited the highest relative density prior to sintering, and the lowest temperature of the start of sintering. Compared to other materials, however, the shrinkage of specimens did not proceed at a high rate; together with alumina, cerium dioxide had the lowest value of maximum shrinkage rate. The interval $<T_1; T_3>$, in which the shrinkage of specimens proceeded at the maximum rate (and which can, more or less, be seen as identical with the sintering region in the open porosity phase), was for ceria ca. 500 °C wide. This range of sintering temperatures corresponds to solid-state sintering [6]. This interval was equally wide only in the case of injection moulded alumina, the other materials sintered in a temperature interval of ca. 400–450 °C.

The temperature at which the compaction of injection moulded ceria began (850 °C) is comparable with the temperature of the sintering start of pressed ceria powders (800–900 °C) of different particle sizes: 10–15 nm, 0.1–0.2 μm and 0.5 μm [7,10]. The lowest temperature of the sintering start (750 °C) was reported in [8] for nanometric (10–14 nm) CeO_2. Thus the temperature of the onset of sintering is not an explicit function of particle size, it also depends significantly on the homogeneity of arrangement and the distribution of particle and pore sizes, degree of agglomerations, etc.

Table 2
Temperature values of shrinkage onset (T_1), temperatures of maximum shrinkage rates (T_2), maximum shrinkage rates (v_{max}) and temperatures of shrinkage slow-down (T_3) established by analysis of shrinkage curves of injection moulded ceria

Heating rate (°C min^{-1})	Sintering temperature/ holding time (°C)/(h)	T_1 (°C)	T_2 (°C)	v_{max} (%/°C)	T_3 (°C)
5	1400/4	851	1258	−0.041	1355
5	1450/3	847	1256	−0.041	1360
5	1500/2	843	1250	−0.040	1356
5	1500/0.67	852	1256	−0.040	1361
10	1500/2	875	1285	−0.039	1390
2	1500/1	830	1219	−0.043	1317

Table 3
Comparison of sintering kinetics of injection moulded ceria with other ceramic materials

Material	Shaping method[a]	$\rho_{rel\ 0}$ (%)	T_1 (°C)	T_2 (°C)	v_{max} (%/°C)	T_3 (°C)
CeO_2	IM	68	850	1255	−0.04	1358
Al_2O_3[b]	IM	64	977	1390	−0.04	1493
Al_2O_3[b]	CIP	65	967	1362	−0.04	1426
ZTA[b]	IM	65	1066	1465	−0.06	1500
ZTA[b]	CIP	67	1043	1450	−0.06	1495
ATZ[b]	IM	64	900	1138	−0.05	1299
ATZ[b]	CIP	65	893	1156	−0.05	1295
ZrO_2[b]	IM	63	904	1273	−0.08	1313
ZrO_2[b]	CIP	49	874	1263	−0.08	1334

[a] IM, injection moulding; CIP, cold isostatic pressing.
[b] Ref. [22].

Fig. 7 gives the temperature and time dependence of relative density of ceria for specimens sintered at a heating rate of 5 °C min^{-1} and at different sintering temperatures. As expected, a higher temperature led to a higher density even with a shorter holding time. In most of the works concerned with the sintering of undoped ceria, nanometric powders were used, which found correspondence in lower sintering temperatures, ranging between 1150 and 1300 °C [7,8,10,12,13]. For the sintering of CeO_2 ceramics from sub-micrometric powders considerably higher temperatures were necessary, ranging from 1450 to 1650 °C [7]. Specimen bodies made of ceria with 0.1–0.2 μm particle sizes reached almost theoretical density at a temperature of 1450–1500 °C (rate of heating 5 °C min^{-1}) while specimens prepared from ceria with 0.5 μm particle size did not exceed 96%TD even at a temperature of 1650 °C [7,10]. The injection moulded sintered ceria used in the present work had after milling a mean particle size of 0.37 μm and its sintering curve resembled that of uniaxially pressed powder with 0.1–0.2 μm particle sizes.

By studying nanometric (10–60 nm) ceria, Nakane et al. [13] established a decrease in density with increasing sintering temperature, namely from 99.8%TD (1150 °C/2 h) to 99.4%TD (1200 °C/2 h) or to 95.7%TD (1300 °C/2 h). Zhou and Rahaman [7,9,10], too, observed on dilatometric curves a drop in the density of specimens made of nanometric (10–15 nm) ceria at a temperature exceeding 1200 °C. This drop in density was accompanied by a decrease in mass and explained by the partial reduction of CeO_2 to Ce_2O_3, both in air atmosphere and in O_2 atmosphere [7]. The released gaseous oxygen led to defects in the microstructure of sintered specimens and cracks on their surface [10]. Sub-micrometric powders (0.15 and 0.5 μm) exhibited smaller reductions in mass than nanometric powder did, their density did not decrease, but points of inflection were observed on dilatometric curves [7,10]. As can be seen from the smooth shapes of the curves in Fig. 7, in the case of our specimens, made of sub-micrometric powder (0.37 μm), there was no such reduction even at a temperature of 1500 °C, which was also corroborated by identical X-ray spectra and identical mass of ceria specimens before and after sintering. The equilibrium of redox reaction $2CeO_2 \longleftrightarrow Ce_2O_3 + \frac{1}{2}O_2$ depends probably on the size of ceria grains. For nanometric (2.1–6.7 nm) ceria powder it was found that the valence change from Ce^{4+} to Ce^{3+} occurred in the case of cerium ions near the surface of particles, and that the conversion of Ce^{4+} to Ce^{3+} increased with decreasing particle size [31]. In Chen and Chen [12] the dilatometric curve of pressed ceria is given, ceria grain size from 1.4–1.5 μm (LIM). The curve is smooth up to temperatures of 1450 °C, which confirms the results obtained in the present work for sub-micrometric ceria, which remained unreduced even at a temperature of 1500 °C. We suppose that the absence of any symptoms of reduction of our ceria ceramics was caused by the relative large size of ceria particles and by using the air atmosphere. With decreasing oxygen partial pressure in the furnace atmosphere the reduction of CeO_2 should increase [32].

Fig. 8 gives an example of injection moulded ceria sintered by the RCS method. With this method, the sintering of the specimen proceeds according to a time-dependence of density, given in advance. The authors of the method declared that with a suitably chosen densification schedule the RCS method led to an optimum sintering cycle with the requirement of maximum specimen density and minimum grain growth [20,21]. In the present work, a densification profile optimized for sub-micrometric alumina [20,21] was used and the result was ceria with a density of 99.5%TD. An analysis of the sintering curve obtained by the TCS method, heating rate 5 °C min^{-1}, sintering temperature 1500 °C (Fig. 7), revealed that to reach a relative density of 99.5%TD a holding time of 40 min at this temperature should be

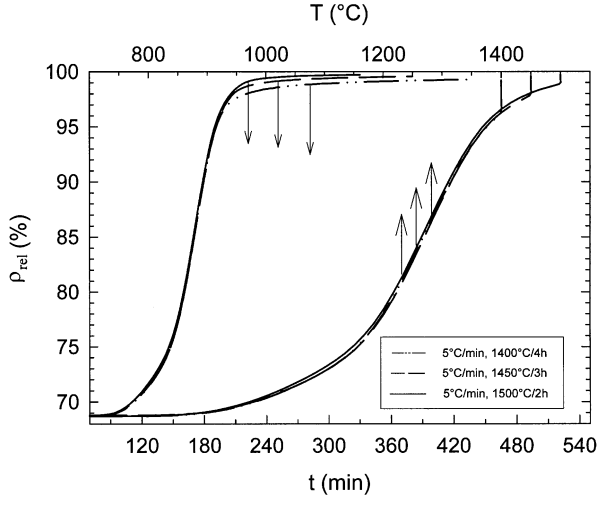

Fig. 7. The dependence of relative density of injection moulded ceria on temperature and time at different sintering temperatures.

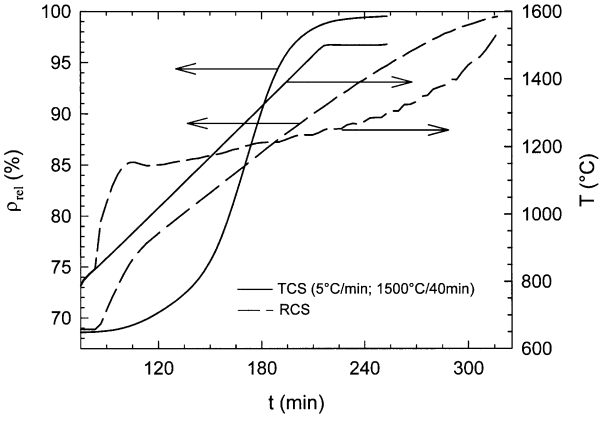

Fig. 8. The dependence of relative density of injection moulded ceria on temperature and time during rate controlled sintering and temperature controlled sintering.

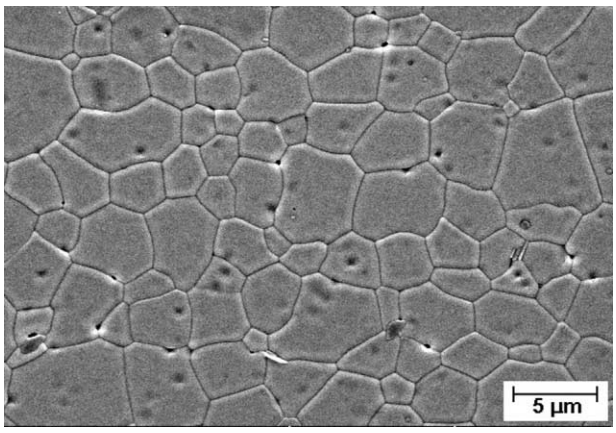

Fig. 9. SEM micrograph of injection moulded ceria sintered at 1500 °C/40 min.

sufficient. The performed sintering experiment at a temperature of 1500 °C for 40 min confirmed the correctness of this assumption and also the high reproducibility of measurements; the final density reached was 99.5%TD (Table 1). It is evident from Fig. 8 that the RCS and TCS heating modes leading to an identical resulting density differed significantly. The following sub-chapter evaluates what effect this had on the microstructure of ceria.

3.5. Microstructure of sintered CeO_2

The structure of all samples was homogeneous and no exaggerated growth of grains was observed. The examples of microstructures of thermally etched sections of CeO_2 ceramics are given in Fig. 9 (sample sintered at 1500 °C/40 min) and Fig. 10 (sample sintered by RCS method). In the structure were sporadic alumina impurities, which are likely to have got into the specimens due to milling with alumina balls. For the milling of this material it will be necessary to use milling bodies made of materials with greater fracture toughness, e.g. ZrO_2 [4,17], or the milling will have to be less intensive since, for example, in Higashi et al. [3] the contamination of ceria powder by milling balls made of alumina was found to be minimum.

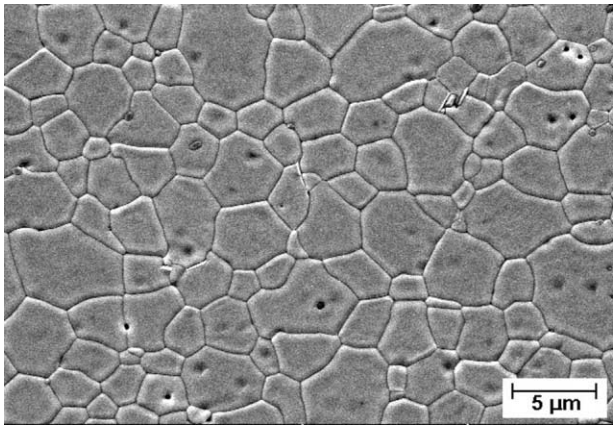

Fig. 10. SEM micrograph of injection moulded ceria sintered by means of rate controlled sintering.

The grain size affects the properties of ceramic products, in the case of ceria it is electrical conductance in particular. With decreasing grain size, ionic conductance decreases and electron conductance of ceria increases [33]. Table 4 gives the grain size of ceria established by the LIM. The grain size increased with increasing sintering temperature (cf. specimens sintered at 1400 °C/4 h, 1450 °C/3 h and 1500 °C/2 h).

After sintering at 1530 °C/2 h, the mean grain size of injection moulded alumina ($d_{50}=0.6$ μm) [34], whose sintering kinetics was similar to that of ceria (Table 3), was 1.6 μm (LIM). From a comparison of this value with the value 4.6 μm for ceria sintered at 1500 °C/2 h (Table 4) it follows that the growth of ceria grains was faster than that of alumina grains. This difference may have been due the addition of 0.05 wt.% of MgO to alumina, which is added just in order to limit the growth of grains. In the case of nanometric ceria it was reported in Rahaman and Zhan [9] that grain growth was suppressed but sintering temperatures increased by the addition of several mol% of cations of greater size than Ce^{2+} (Ca^{2+}, Nd^{3+} and Y^{3+}).

A comparison of the grain size of ceria with that of injection moulded ZrO_2 (stabilized with 3 mol% of Y_2O_3), which had similar rheological properties as ceria (Section 3.2) and is, similar to ceria, an ionic conductor, again shows a very fast growth of ceria grains. ZrO_2, whose initial particle size was 0.1 μm, had after sintering at 1500 °C/2 h a mean grain size (LIM) of only 0.4 μm [34]. It can be seen from Figs. 9 and 10 and from Table 4 that applying the RCS method did not yield a microstructure of smaller grain size than when applying the TCS method with optimized holding time on the sintering temperature. The difference in the mean grain size was within the measuring error. These results thus did not confirm the results obtained in the past on sub-micrometric alumina [20,21,34] and sub-micrometric ZrO_2 [34], where the RCS method led to microstructures with grains that were 40 to 400% smaller than in the case of the TCS method. In the works quoted, however, the

Table 4
Mean grain size of sintered ceramic materials (D) established by linear intercept method, inclusive of standard deviations (s), number of grains measured (n) and maximum grains found (D_{max})

Sintering temperature/ holding time (°C)/(h)	ρ_f (%)	D (μm)	s (μm)	n (–)	D_{max} (μm)
1400/4	99.28	2.68	0.35	367	8.74
1450/3	99.57	3.94	0.49	251	9.99
1500/2	99.71	4.60	0.76	218	14.49
1500/0.67	99.52	2.96	0.33	224	8.33
RCS	99.51	2.76	0.24	241	8.00

TCS method was not optimized as was the case in the present work.

4. Conclusion

It has been verified that using the technology of injection moulding, compact ceria-based ceramics can be prepared. The application of commercial ceria powder required treating the ceria by dry ball-milling to submicrometric level of particle size. Using alumina balls led to the ceramics being contaminated with aluminium oxide. Sintering the ceria to relative densities of more than 99% was possible already at a sintering temperature of 1400 °C. The maximum final relative density (99.8%) was achieved by sintering at a heating rate of 2 °C min^{-1} and a holding time of 1 h at 1500 °C. Using heating rates higher than 5 °C min^{-1} had an adverse effect on the density obtained. Applying the method of rate-controlled sintering did not lead to any reduction in the grain size when compared with the optimized method of temperature-controlled sintering. No reduction of CeO_2 ceramics was observed during all sintering experiments.

References

[1] A. Tsoga, A. Naoumidis, W. Jungen, D. Stöver, Processing and characterization of fine crystalline ceria gadolinia-yttria stabilized zirconia powders, J. Eur. Ceram. Soc. 19 (1999) 907–912.
[2] H. Yoshida, K. Miura, J. Fujita, T. Inagaki, Effect of gallia addition on the sintering behavior of samaria-doped ceria, J. Am. Ceram. Soc. 82 (1) (1999) 219–221.
[3] K. Higashi, K. Sonoda, H. Ono, S. Sameshima, Y. Hirata, Synthesis and sintering of rare-earth-doped ceria by oxalate coprecipitation method, J. Mater. Res. 14 (3) (1999) 957–967.
[4] J. Van herle, T. Horita, T. Kawada, N. Sakai, H. Yokokawa, M. Dokiya, Fabrication and sintering of fine yttria-doped ceria powder, J. Am. Ceram. Soc. 80 (4) (1997) 933–940.
[5] J. Van Herle, T. Horita, T. Kawada, N. Sakai, H. Yokokawa, M. Dokiya, Sintering behaviour and ionic conductivity of yttria-doped ceria, J. Eur. Ceram. Soc. 16 (1996) 961–973.
[6] C. Kleinlogel, L.J. Gauckler, Sintering and properties of nanosized ceria solid solutions, Solid State Ionics 135 (2000) 567–573.
[7] Y.C. Zhou, M.N. Rahaman, Hydrothermal synthesis and sintering of ultrafine CeO_2 powders, J. Mater. Res. 8 (7) (1993) 1680–1686.
[8] Y. Zhou, R.J. Philips, J.A. Switzer, Electrochemical synthesis and sintering of nanocrystalline cerium(IV) oxide powders, J. Am. Ceram. Soc. 78 (4) (1995) 981–985.
[9] M.N. Rahaman, Y.C. Zhou, Effect of solid solution additives on the sintering of ultra-fine CeO_2 powders, J. Eur. Ceram. Soc. 15 (1995) 939–950.
[10] Y. Zhou, M.N. Rahaman, Effect of redox reaction on the sintering behavior of cerium oxide, Acta Mater. 45 (9) (1997) 3635–3639.
[11] M.N. Rahaman, R.E. Dutton, S.L. Semiatin, Effect of solid solution additives on the densification and creep of granular ceramics, Acta Mater. 45 (7) (1997) 3017–3027.
[12] P.L. Chen, I.W. Chen, Reactive cerium(IV) oxide powders by the homogenous precipitation metho, J. Am. Ceram. Soc. 76 (6) (1996) 1577–1583.
[13] S. Nakane, T. Tach, M. Yoshinaka, K. Hirota, O. Yamaguchi, Characterization and sintering of reactive cerium(IV) oxide powders prepared by hydrazine method, J. Am. Ceram. Soc. 80 (12) (1997) 3221–3224.
[14] H. Inaba, T. Nakajima, H. Tagava, Sintering behaviors of ceria and gadolinia-doped ceri, Solid State Ionics 106 (1998) 263–269.
[15] A. Rosen, H.K. Bowen, Influence of various consolidation techniques on the green microstructure and sintering behaviour of alumina powders, J. Am. Ceram. Soc. 71 (11) (1998) 970–977.
[16] J. Zheng, J.S. Reed, Effects of particle packing characteristics on solid-state sintering, J. Am. Ceram. Soc. 72 (5) (1989) 810–817.
[17] J. Van Herle, T. Horita, T. Kawada, N. Sakai, H. Yokokawa, M. Dokiya, Oxalate coprecipitation of doped ceria for tape casting, Ceram. Int. 24 (1998) 229–241.
[18] I. Zhitomirsky, A. Petric, Electrolytic and electrophoretic deposition of CeO_2 films, Mater. Lett. 40 (1999) 263–268.
[19] J.A. Brydson, Flow Properties of Polymer Melts, George Goodwin, London, UK, 1981.
[20] H. Palmour III, M.L. Huckabee, US patent 3 900 542, 19 August 1975.
[21] M.L. Huckabee, H. Palmour III, Rate controlled sintering of fine-grained Al_2O_3, Am. Ceram. Soc. Bull. 51 (1976) 574–576.
[22] K. Maca, H. Hadraba, J. Cihlar, Study of sintering of ceramics by means of high-temperature dilatometry, Ceramics-Silikáty 42 (4) (1998) 151–158.
[23] R.E.F.Q. Nogueira, M.J. Edirisinghe, D.T. Gawne, Selection of a powder for ceramic injection moulding, J. Mater. Sci. 27 (1992) 6525–6531.
[24] C.W. Macosko, Rheology: Principles, Measurements, and Applications, VCH Publishers, New York, 1993.
[25] J. Cihlar, Z. Racl, Rheology of thermoplastic polymer-ceramic mixtures, in: Proceedings of the PIM98, The Pennsylvania State University, 1998, pp. 69–78.
[26] M. Trunec, P. Dobsak, J. Cihlar, Effect of powder treatment on injection moulded zirconia ceramics, Eur. Ceram. Soc. 20 (2000) 859–866.
[27] M.L. Gupta, S. Sigh, Thermal expansion of CeO_2, Ho_2O_3, and Lu_2O_3 from 100° to 300 °K by an X-ray method, J. Am. Ceram. Soc. 53 (12) (1970) 663–665.
[28] M. Mogensen, N.M. Sammes, G.A. Tompsett, Physical, chemical and electrochemical properties of pure and doped ceria, Solid State Ionics 129 (2000) 63–94.
[29] F. Brezina, et al., Chemical Tables of Anorganic Compounds, SNTL, Praha, CR, 1986.
[30] D.R. Lide, CRC Hanbook of Chemistry and Physics, 72nd Edition, CRC Press, USA, 1992.
[31] S. Tsunekawa, R. Sivamohan, S. Ito, A. Kasuya, T. Fukuda, Structural study on monosize CeO_{2-x} nano-particles, Nano Structured Mater. 11 (1) (1999) 141–147.
[32] O. Toft Sorensen, Thermodynamic studies of the phase relationship of nonstoichiometric cerium oxides at higher temperatures, J. Solid State Chem. 18 (1976) 217–233.
[33] A. Tschöpe, E. Sommer, R. Birringer, Grain size-dependent electrical conductivity of polycrystalline cerium oxide I. Experiments, Solid State Ionics 139 (2001) 255–265.
[34] K. Maca, H. Hadraba, J. Cihlar, Study of sintering of oxide ceramics at constant rate of heating and by means of rate controlled sintering method, in: G. Mueller (Ed.), Ceramics—Processing, Reliability, Tribology and Wear, Vol. 12, Wiley-VCH, Weinheim, 2000, pp. 161–166.